doi:10.14311/ppt.2025.1.34
Plasma Physics and Technology **12**(1):34–39, 2025

INVESTIGATION OF DETECTING DC SERIES ARCS WITH SHORT GAPS TO SIMULATE FAILURE CONDITIONS IN ACTUAL LOW-VOLTAGE DC FACILITIES

M. Iwata[a,*], N. Nishiyama[a], Y. Yokomizu[a], N. Kodama[a], A. Nakamura[a], K. Ishikawa[a], T. Sakai[b], M. Tsukahara[b], A. Miyamoto[b]

[a] *Nagoya University, Furo-cho, Chikusa, Nagoya, Aichi 464-8603, Japan*

[b] *Nitto Kogyo Corporation, 2201 Kanihara, Nagakute, Aichi 480-1189, Japan*

[*] iwata.mikimasa.x4@f.mail.nagoya-u.ac.jp

Abstract. Direct current (DC) facilities are increasing with the spread of renewable energy such as photovoltaic power generation. DC series arc may occur in poor contact or disconnecting in the facilities and cause fire incidents. This paper presents DC series arc generation experiments in air considering actual failure conditions, and Wavelet transformation analysis of the measured current waveform. Using the obtained results, a method of detection of arc generation in low-voltage DC facilities is proposed.

Keywords: renewable energy, low-volage DC facility, short-gap arc, detection method of arc generation.

1. Introduction

As renewable energy sources are becoming widely used to achieve carbon neutrality by 2050, direct current (DC) technology is used in power transmission facilities from photovoltaic (PV) power generation facilities. This is because DC electricity is generated by PV power generation equipment.

When a fault occurs (e.g., circuit is shorted or opened) in the DC system, an arc discharge generated due to the fault tends to continue to burn because DC has no cyclical natural current zero point [1]. Since the temperature of arcs is quite high, e.g., around 10,000 K [2], the arcs that continue burning inside or near DC facilities can cause fires of the facilities [3–7]. When a short-circuit fault occurs in DC facilities, the fault is easily detected because the DC circuit is shorted without passing through loads in the circuit, and the value of flowing current increases significantly. However, when a disconnection or poor contact of conductor wire occur in DC facilities, the circuit is opened with a short gap and a fault arc is generated. The fault behaviour is difficult to detect since the current flows through the loads in the circuit and does not change significantly. In this case, the arc is called "series arc" because it is generated as connecting in series with load in the DC circuit.

In a study on detecting DC series arcs in PV system, a Fourier transformation was performed on the PV panel-to-panel voltage [7]. This method requires measuring the voltage at each PV panel, and the time of arc occurrence cannot be known because information regarding the time is lost due to Fourier transformation of the voltage waveform. Therefore, in our previous studies [8–10] we tried to identify the time of arc occurrence using Wavelet transformation which is one of the frequency analysis methods and can preserve time-domain information. And we focused on the waveform of the current, which is measured in actual DC facilities, and performed a Wavelet transformation of current waveforms.

In this paper, Wavelet transformation was applied to the current waveform as in our previous studies. The arc is generated at a short gap of 0.4 mm, 5 mm, and 10 mm between copper electrodes in air, assuming a failure in an actual facility. We attempted to detect the generation of arcing by focusing on the temporal variation of the signal obtained with an analysis frequency of 1 kHz to 10 kHz in the Wavelet transformation.

2. Arc generation experiments

2.1. Experimental conditions

As shown in Figure 1, an arc generation equipment was connected in series to a DC power supply. The arc equipment has an upper electrode and a lower electrode, each of which is a 10 mm diameter copper electrode with a hemispherical tip. An arc was generated in air by flowing the current while the lower electrode was raised and in contact with the upper electrode and then letting the lower electrode fall. The lower electrode was dropped until the distance between the electrodes was 0.4 mm, 5 mm, and 10 mm. The distance between the electrodes was measured using potentiometers on the upper and lower electrodes, the DC power supply voltage and the voltage between electrodes were measured using voltage probes, and the current was measured using a shunt resistor. These measurements were performed before and after the arc generation. The DC power supply voltage was changed 100 V, 200 V, and 300 V. In each case, the value of circuit resistor was adjusted so that the

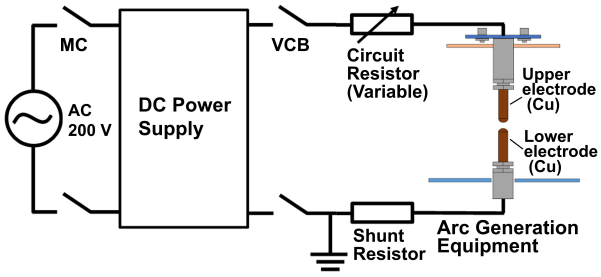

Figure 1. Experimental circuit for arc generation in air.

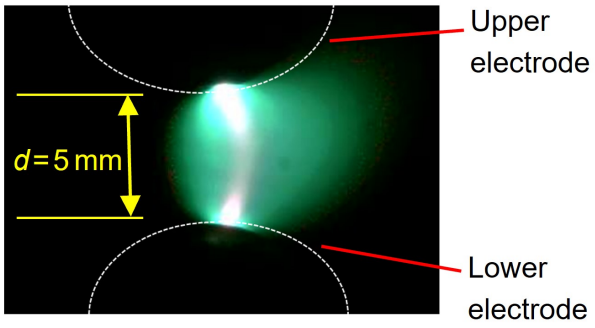

Figure 2. An arc image observed using high speed video camera [10]. (Observation speed: 1000 fps, Shutter speed: 1/10000 s^{-1}, Filter: ND8)

current was a constant 40 A. Six experiments were carried out under each condition.

2.2. Experimental results

Figure 2 shows an example of an image of the arc generated between upper and lower electrodes observed using a high-speed video camera. The image was obtained when the distance between electrodes d was 5 mm. It is thought that the current flows mainly in the arc column with high brightness. The arc is curved slightly to the right, and this may be due to the movement of the arc spot on the electrode and electromagnetic forces on the arc column.

Figure 3 shows an example of experimental results for inter-electrode distance d of 0.4 mm, 5 mm, and 10 mm when the DC power supply voltage is 100 V. Figures 3a and 3b show the time-dependence of the voltage between electrodes (inter-electrode voltage) and the current, respectively. In all conditions, a current of 40 A was being applied to the contacting upper and lower electrodes, and at the time 0 ms the lower electrode was dropped, and an arc was generated, increasing the inter-electrode distance up to 0.4 mm, 5 mm, and 10 mm.

In the waveform of the voltage between electrodes in Figure 3a, a voltage of about 16 V appears immediately after the arc is generated at 0 ms. This is almost the same value as the measured value [11] of the electrode drop voltage in air arcs generated between copper electrodes. Thereafter, the voltage between the electrodes increased as the distance between the electrodes increased, reaching e.g., 35 V to

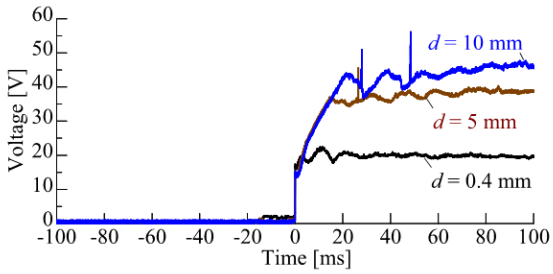

(a) . Inter-electrode voltage

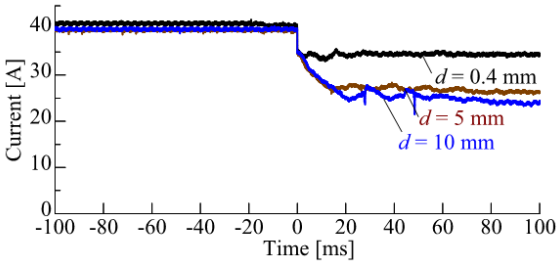

(b) . Current

Figure 3. Examples of waveforms obtained by arc generation experiments. (DC power supply voltage: 100 V)

40 V after 15 ms in the case for $d = 5$ mm. In the current waveforms shown in Figure 3b, the current decreases in a staircase-like pattern immediately after the opening of the electrodes at 0 ms in all cases, which can be attributed to the electrode drop voltage described above. In other words, the current is considered to have decreased rapidly due to the appearance of an electrode drop voltage described above in the DC circuit at the instant of arc generation. After the generation of the arc, the current decreases slowly and becomes almost constant after e.g., 15 ms in the case for $d = 5$ mm, but during the arcing, the current is found to be unstable and changes slightly. Focusing on the minute changes in the current, a Wavelet transformation analysis of the current waveform is performed to detect the arc occurrence, and the details of the analysis method and the results are described in the next chapter.

3. Wavelet transformation of current waveforms

3.1. Analysis method using Wavelet transformation

As described in the experimental results in Section 2.2, the current waveform was unstable and varied slightly during arc generation. Since current waveform data can be easily measured in actual DC facilities, we focused on these minute changes in current during arc generation and performed frequency analysis of the current waveform. We considered that a time-by-time frequency analysis would be effective. As described in Section 1, in a study [7], a Fourier transformation was performed on the PV panel-to-panel voltage to

detect DC series arcs in PV system. In this method, the time of arc occurrence cannot be known because information regarding the time is lost due to Fourier transformation of the voltage waveform. We therefore performed the analysis using the Wavelet transformation which is one of the frequency analysis methods and can preserve time-domain information. The continuous Wavelet transformation for the input signal $x(t)$ is expressed as W in amplitude as in the following equation

$$W = \frac{1}{\sqrt{|a|}} \int_{-\infty}^{+\infty} x(t)\psi^* \left(\frac{t-b}{a}\right) \mathrm{d}t. \tag{1}$$

The function $\psi(t)$ is a mother wavelet. The value a is a stretching parameter and is related to the frequency f by using the peak frequency f_p as follows

$$f = \frac{f_p}{a}, \tag{2}$$

b in equation (1) is the position parameter, and continuously changing of this value can make a time-by-time frequency analysis [12].

In this paper, Morse Wavelets are used for the mother wavelet $\psi(t)$. In Morse Wavelets, there are β and γ parameters, which represent symmetry and damping, respectively [13]. The peak frequency f_p described above can be expressed using these parameters in the following equation

$$f_p = \frac{1}{2\pi} \left(\frac{\beta}{\gamma}\right)^{\frac{1}{\gamma}}. \tag{3}$$

In this case, values of $\beta = 20$ and $\gamma = 3$ were used, resulting in a peak frequency of $f_p = 0.30\,\mathrm{Hz}$. The Morse Wavelet in this case is expressed by the following equation [14]

$$\psi_{20,3}(t) = a_{20,3}(-j)^{20} \frac{1}{2} \frac{1}{3^{\frac{1}{3}}} \frac{\mathrm{d}^{20}}{\mathrm{d}t^{20}} \left\{ \mathrm{Hi}\left(\frac{jt}{3^{\frac{1}{3}}}\right) \right\} \tag{4}$$

where $a_{20,3}$ is the normalization constant, $\mathrm{Hi}(z)$ is the Airy function shown by

$$\mathrm{Hi}(z) = \frac{1}{\pi} \int_0^{\infty} \exp\left(\frac{-u^3}{3} + zu\right) \mathrm{d}u. \tag{5}$$

A figure of the time-dependence of the amplitude W for each frequency, with b as the time component on the horizontal axis and the frequency f on the vertical axis, is called a scalogram, and allows the user to visually understand the time transition of the frequency components in the signal to be analyzed. However, the signal is not detected correctly at the beginning and end of the signal, and a conic sphere of influence appears with an abnormally high amplitude value.

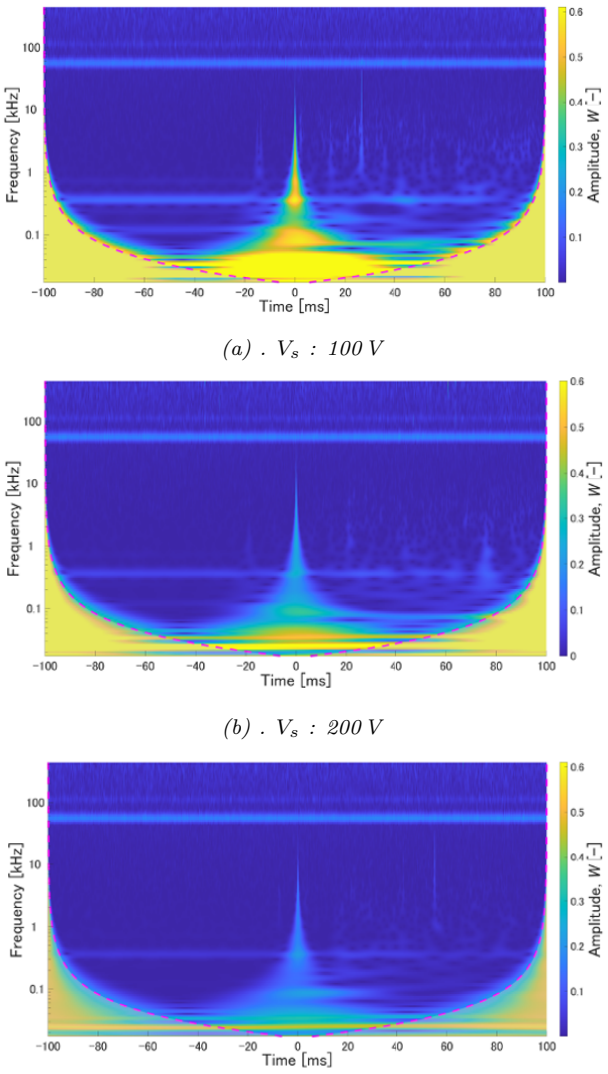

(a) . V_s : 100 V

(b) . V_s : 200 V

(c) . V_s : 300 V

Figure 4. Scalograms obtained by Wavelet transformation of current waveforms for different DC power supply voltage V_s [10]. (Inter-electrode distance d: 5 mm)

3.2. Scalogram obtained by Wavelet transformation of current waveform

Scalograms of the currents were obtained using the method presented in the previous section for frequencies ranging from 0.018 kHz to 430 kHz. The scalograms are shown in Figure 4.

Figure 4a shows a scalogram obtained by Wavelet transformation of the current waveform at a DC power supply voltage of 100 V. The area below the dotted red line is the conic sphere of influence and is not considered here. Near 50 kHz, an almost constant amplitude appears for all time ranges, which is due to high-frequency noise superimposed on the current. At 0 ms, a spire-shaped amplitude distribution with a magnitude of about 0.5 appears in the frequency region lower than 10 kHz, which is due to the current decrease in a staircase-like pattern at 0 ms (the

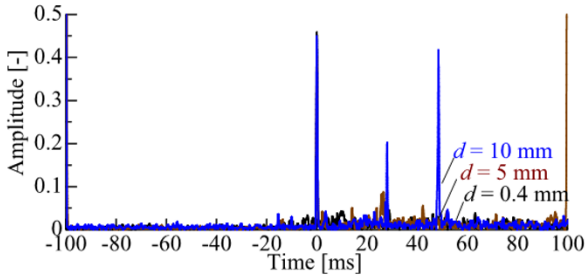

Figure 5. Time-dependence of amplitude of the signal obtained from scalogram. (DC power supply voltage: 100 V, Analysis frequency: 5 kHz)

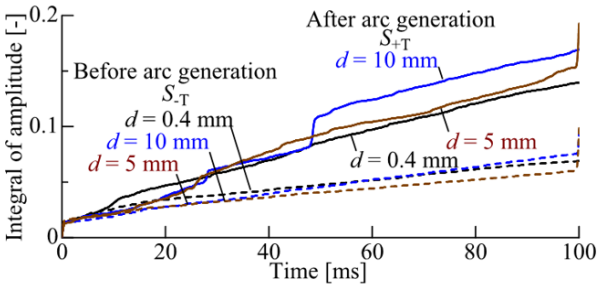

Figure 6. Time-integrated amplitude of the signal before and after arc generation. (DC power supply voltage: 100 V, Analysis frequency: 5 kHz)

moment of an arc generation) as already shown in Figure 3b. In addition, an amplitude with a magnitude of about 0.1 appears in the frequency range of 1 kHz to 10 kHz at times after 0 ms during arc generation, although such amplitudes are not often seen before 0 ms at which the arc is not generated.

Figures 4b and 4c show the scalograms for a DC power supply voltage of 200 V and 300 V, respectively. In both cases, the higher the supply voltage, the lower the amplitude at 0 ms, and the lower the amplitude during arc generation. While the scalograms can graphically show time-by-time frequency analysis, quantitative analysis is difficult. Therefore, quantitative analysis of the scalograms described above is performed in the next section.

3.3. Time variation of the amplitude of the scalogram

In order to quantitatively analyze the results of the scalogram obtained by the Wavelet transformation of the current waveform, we focused on certain analysis frequencies. To investigate the amplitude of the scalogram appearing in the analysis frequency range of 1 kHz to 10 kHz during arc generation, we investigated the change in amplitude over time at the frequency 1 kHz, 5 kHz, and 10 kHz, respectively. In our previous studies, it was clarified that 5 kHz was the best as the analysis frequency considering the intensity of the amplitude and the time resolution of analysis [11].

Figure 5 shows an example of the amplitude variation over time at the analysis frequency 5 kHz. The amplitudes with magnitudes exceeding 0.02 do not often appear between -100 ms and 0 ms, at which the arc is not generated. This is because the current is constant before the arc generation as shown in Figure 3b. At 0 ms, there is an amplitude with a high value. The magnitude corresponds to the magnitude of the staircase-like current change at time 0 ms described in Section 2. At times after 0 ms during arc generation the amplitudes with magnitudes exceeding 0.02 often appear. Taking advantage of this feature, we will attempt to detect the generation of arcing in the next section.

3.4. Analysis of the amplitude of a scalogram by time integration

In the previous chapter, it is found that after the arc generation, amplitudes appear that are not observed before the generation of the arc. In order to utilize this feature to detect the generation of the arc, we compared the time-integrated changes in amplitude before and after the generation of arcing. In this section, the amplitude variation over time is investigated for an analysis frequency of 5 kHz, considering the intensity of the amplitude and the time resolution of analysis as described in the previous chapter.

The time integrated value of the amplitude W up to time after the generation of the arc, $S_{+\mathrm{T}}$, can be expressed by the following equation

$$S_{+\mathrm{T}} = \int_0^T W \mathrm{d}t. \tag{6}$$

The integral value $S_{-\mathrm{T}}$ of the amplitude before arc generation can be expressed by the following equation

$$S_{-\mathrm{T}} = \int_{-T}^0 W \mathrm{d}t. \tag{7}$$

Figure 6 shows $S_{+\mathrm{T}}$ and $S_{-\mathrm{T}}$ as solid and dashed lines, respectively. Since $S_{-\mathrm{T}}$ is the time-integrated value of the amplitude when the time is negative before 0 ms as shown in equation (7), the time on the horizontal axis in Figure 6 is expressed in absolute value.

As can be seen from this figure, as time increases, $S_{-\mathrm{T}}$ gradually increases linearly, while $S_{+\mathrm{T}}$ increases with an increasing slope of the curve in some areas. This is because, as shown in Figure 5, there are few high amplitudes before 0 ms, but there are many high amplitudes after 0 ms.

Based on these results, it is considered that the amplitude obtained by Wavelet transformation of the current waveform after the arc generation is relatively high, and the time-integrated of the amplitude $S_{+\mathrm{T}}$ becomes higher. As a result, $S_{+\mathrm{T}}$ is higher than $S_{-\mathrm{T}}$ and the difference between them tends to be larger over time.

3.5. Proposal of a detection method of arc generation in low-voltage DC facilities

By using the results obtained above, it is considered that the generation of arcs can be detected as following procedure.

1. Wavelet transformation of the waveform of the current, which is measured in actual DC facilities, is carried out.

2. Scalograms are obtained by Wavelet transformation of current waveforms, and waveforms regarding time-dependence of amplitude of the signal are obtained from scalograms for an analysis frequency, e.g., 5 kHz.

3. If a relatively high signal amplitude is detected at a certain time, the amplitudes before and after that time (e.g., 100 ms) are integrated over time.

4. If the two values above are compared and a significant difference is found, the generation of an arc at that time can be detected.

In order to apply the above method to actual DC facilities, we will expand the data by examining the case of different electrode distances, etc., to confirm the effectiveness of the proposed detection method of arc generation.

4. Conclusions

With a view to the continued increase in DC technology, our studies aim to develop methods for detecting DC series arc faults which occur by disconnection or poor contact in DC facilities. In this paper, the arc generation experiments were carried out at 0.4 mm, 5 mm, and 10 mm distance between copper electrodes in air. And, to identify the time of arc generation Wavelet transformation was used, which is one of the frequency analysis methods and can preserve time-domain information. And we focused on the waveform of the current, which is measured in actual DC facilities, and performed a Wavelet transformation of the current waveform. After that, waveforms regarding time-dependence of amplitude of the signal are obtained by the Wavelet transformation for analysis frequency 5 kHz, which is used considering the intensity of the amplitude and the time resolution of analysis.

As a result, it was found that there were amplitudes with a magnitude exceeding 0.02 after arc generation, which did not often appear before arc generation. By comparing the time-integrated values of the amplitudes before and after arc generation, we found the difference in value was caused by the arc. By taking advantage of the difference, it is considered that the generation of arcing can be detected.

In the future, we will expand the data by examining the case of different electrode distances, etc., to confirm the effectiveness of the proposed detection method of arc generation. In addition, from the phenomenological aspect we will also investigate in detail to find the cause of the minute fluctuations in the current waveforms subjected to the Wavelet transformation.

References

[1] M. Seeger, F. Macedo, U. Riechert, et al. Trends in high voltage switchgear research and technology. *IEEJ Transactions on Electrical and Electronic Engineering*, 20:322–338, 2025. doi:10.1002/tee.24244.

[2] Y. Kito, T. Sakuta, and A. Kamiya. Thomson scattering of laser light from a high pressure air arc discharge and its application to electron density measurement. *J. Phys. D: Appl. Phys.*, 17:2283–2290, 1984. doi:10.1088/0022-3727/17/11/015.

[3] H. Laukamp, G. Bopp, R. Grab, et al. PV fire hazard - analysis and assesment of fire incidents. In *Proc. 28th European Photovoltaic Solar Energy Conference and Exhibition (EU PVSEC 2013)*, pages 1–8, 2013. doi:10.4229/28thEUPVSEC2013-5BV.7.71.

[4] M. C. Falvo and S. Capparella. Safety issues in PV systems: Design choices for a secure fault detection and for preventing fire risk. *Case Studies in Fire Safety*, 3:1–16, 2015. doi:10.1016/j.csfs.2014.11.002.

[5] K. M. Armijo, J. Johnson, R. K. Harrison, et al. Quantifying photovoltaic fire danger reduction with arc-fault circuit interrupters. *Progress in Photovoltaics: Research and Applications*, 24:507–516, 2016. doi:10.1002/pip.2561.

[6] L. Fiorentinia, L. Marmob, E. Danzi, and V. Puccia. Fire risk assessment of photovoltaic plants. A case study moving from two large fires: from accident investigation and forensic engineering to fire risk assessment for reconstruction and permitting purposes. *CHEMICAL ENGINEERING TRANSACTIONS*, 48:427–432, 2016. doi:10.3303/CET1648072.

[7] H.-P. Park, M. Kim, J.-H. Jung, and S. Chae. Arc fault detection method for PV systems employing differential power processing structure. *IEEE Transactions on Power Electronics*, 36(9):9787–9795, 2021. doi:10.1109/TPEL.2021.3061968.

[8] N. Nishiyama, M. Iwata, Y. Yokomizu, et al. Wavelet analysis for detecting low-voltage DC short-gap arc under different voltage conditions.(in Japanese). In *Proc. the 2024 Annual Meeting of the IEEJ*, number 6-038, 2024.

[9] N. Nishiyama, M. Iwata, Y. Yokomizu, et al. Fundamental study on low voltage DC series arc detection method -wavelet analysis of currents supposing faults in DC facilities.(in Japanese). In *Proc. 2024 Annual Conference of Power and Energy Society of the IEEJ*, number 238, 2024.

[10] M. Iwata, N. Nishiyama, Y. Yokomizu, et al. A proposal for a detection method of short-gap arcs generated in low-voltage DC facilities. In *Proc. IEEJ PES - IEEE PES Thailand Joint Symposium 2025*, number TJS-25-007, 2025.

[11] Y. Yokomizu, T. Matsumura, R. Henmi, and Y. Kito. Total voltage drops in electrode fall regions of argon and air arcs in current range from 10 to 20 000 A. *J. Phys. D: Appl. Phys.*, 29:1260–1267, 1996. doi:10.1088/0022-3727/29/5/020.

[12] P. S. Addison. *Illustrated Wavelet Transformation Handbook, eds. S. Shin, K. Nakano*. Asakura Publishing, 2005.

[13] MathWorks. Morse Wavelet. [access: 2025/06/15]. arXiv:https://jp.mathworks.com/help/wavelet/ug/morse-wavelets.html.

[14] J. M. Lilly and S. C. Olhede. Higher-order properties of analytic wavelets. *IEEE Trans. on Signal Processing*, 57(1):146–160, 2009. doi:10.1109/TSP.2008.2007607.